Modelling a C-type Flare Observed in Microwaves and Hard X-rays

E.J. Schmahl and M.R. Kundu

University of Maryland

Astronomy Program

and

B.R. Dennis

Laboratory for Astronomy and Solar Physics

GSFC

To be submitted to the Proceedings of the

Max '91 Workshop

June 1988

Abstract

Modelling a C-type Flare Observed in Microwaves and Hard X-rays

Using the Very Large Array at 6 and 20 cm wavelength and the Hard X-ray Burst Spectrometer on the Solar Maximum Mission, we have observed a two-ribbon flare from the onset phase through the maximum and decline on November 14, 1981. Because of the extensive size of the microwave source and the gradual variations in hard x-rays whose spectrum becomes progressively flatter with time, the flare is classified as a C-type flare. Considering the hardening of the x-ray spectrum and its non-impulsive nature, we invoke a coronal trap model for the energetic electrons. The microwave emission is easily accounted for by gyrosynchrotron radiation from mildly relativistic electrons. We have found that the source must be optically thick at 20 cm during the maximum phase, but as the source evolved toward an optically thin regime, the intensity decreased while the degree of circular polarization increased. In an initial homogenous model, we found that the computed microwave spectrum was too narrow to match the patrol spectrum from 606 to 15400 MHz. Because of this fact and the observed limbward displacement of the 20 cm emission from the H α emission, we were led to an inhomogeneous model of the magnetic field which traps the electrons. In our new model, the magnetic field consists of a dipolar arcade bridging the H α ribbons, and extending to heights of order 4 to 5 x 10^4 km. The variation of the magnetic field strength from footpoints to apex causes the gyrosynchrotron spectrum to be broader.

Since the height of the arcade, its width and footpoint field strengths are known from the Hα , 20 cm, and magnetograph observations, there are relatively few free parameters in the model.

We present and discuss preliminary conclusions regarding the electron distributions producing the hard x-rays and the microwaves, and the suitability of this model for C-type flares.

Modelling a C-type Flare Observed in Microwaves and Hard X-rays

The two-ribbon, class 2B flare of 1981 November 14 was observed by HXRBS in x-rays with energies from 31 to 539 keV and in microwaves at the VLA and the patrol telescopes at Palehua. Fig. 1 shows the time profiles of x-rays and the microwave flux. By combining the microwaves with the hard x-rays we shall attempt to distinguish between the thin and thick target models, estimate the range of coronal magnetic fields in the trapping loops, and estimate the degree of pitch angle anisotropy in the trapped electrons.

The HXRBS channels were fitted to a power law and the index γ plotted as a function of time. The time profile (Fig. 2) shows that the spectrum hardened from γ= 4.0 to about γ=3.3 starting from just before the x-ray maximum and continuing until at least 15 minutes afterwards. Because of the spectral hardening, and also because of the large area of the flare, this flare is classified as a type C, following the characterization of Tanaka, (IAU Symp. No. 71, 1983) and Tsuneta et al., (Ap. J. 280, 887, 1984).

The microwave patrol data were fitted to a double power law function, and the upper index α plotted as a function of time. Although this index is not strictly equal to the high frequency index of the microwaves, the profile shows that the spectrum hardened significantly and monotonically through the flare.

To show the evolution of the microwave spectral index, we have plotted the 8800 MHz flux against the 15400 MHz flux (Fig. 3) This shows that, from shortly before the main hard x-ray peak to well after, the spectrum hardens steadily with the logarithmic slope α decreasing from -1.3 (at 22:02) to -0.5 (at 22:20). This index differs somewhat from that derived by the double power law fit (Fig. 2), but shows the same qualitative behavior. In general, the microwave indices imply electron energy indicies δ which are around 2.2-2.7, which argues for thin target emission.

We have made numerous snapshot maps of the flare at both 6 and 20 cm, but focus on the period after the hard peak at 22:03 UT. Fig. 4 shows the 6 cm I and V VLA maps at 22:05 and 22:11 UT. Note the two oppositely polarized peaks in the 6 cm map; these appear to straddle the Hα filament in the flaring region. Figure 5 shows the 20 cm I and V VLA maps at the same times as the previous 6 cm maps. The 20 cm intensity source is single, with its location centered between the two 6 cm peaks (Fig. 4). The polarization map shows that the edges of the source are polarized in the same sense as the two 6 cm sources. From the VLA maps alone, it is apparent that the burst source must be a large loop overlying the neutral line, and this is borne out by comparison with Hα photographs from Big Bear (courtesy of H. Zirin).

When the 20 cm map for 22:40 UT is overlain on the Hα photograph, the similarity is striking (Fig. 6). We have made a 33" shift in position (away from the limb) of the 20 cm map (see dashed arrow) to align the Hα ribbons and the maxima of the microwave map. The shift corresponds to a projection effect with the height of the 20 cm sources 4-5 x 10^4 km above the Hα ribbons.

One of the most important features of the microwave spectrum is its large width (Fig. 7). Note the extreme breadth of the spectrum throughout the flare. For comparison, compare the overlay of a gyrosynchrotron spectrum of a homogeneous source. The breadth indicates that the source contains a wide range of magnetic field strengths, presumably in a system of loops trapping the electrons.

To account for the observed spectrum, we have computed gyrosynchrotron emission as a function of frequency from a model dipole loop with parameters esimated from the observations (Fig. 8). The magnetic field is that due to a buried linear dipole. The magnetic field strength at the footpoint is specified as a free parameter, but may be estimated from magnetograph observations.

We have computed gyrosynchrotron spectra from the model loop

system for a wide range of parameters, keeping the observable constraints in mind. The crosses in Fig. 9 show the Palehua flux at 22:08:00 UT. The highest curve is the flux integrated over the entire loop, while the lower curves are the flux at selected points from the center outward toward the footpoints. We allowed the pitch angle distribution to depart from anisotropy, using the form:

$N(\phi)=(\sin(\phi))^p$, where p=0 corresponds to the isotropic case. For this kind of distribution, Parker (Phys. Rev. 107, 924, 1957) showed that the density of electrons in the loop is inversely proportional to the pth power of the magnetic field at that point.

Conclusions:

1. The hard x-ray spectrum hardens with time, and when modeled in terms of thin and thick target bremsstrahlung, gives energy indices of 3.1-2.7 and 4.6-4.3 (respectively). The microwave spectrum also hardens with time. The microwave spectral index (which depends somewhat on the method used to define it) corresponds more closely to the thin target model than the thick.

2. As evidenced by the broad microwave spectrum, the microwaves are generated in a set of regions with widely ranging magnetic field strengths.

3. The VLA maps show that these regions are a continuous, smooth system, rather than isolated sources: the 6 cm source is double, spanning the neutral line, and the 20 cm source is single with polarized edges, also spanning the neutral line. The simplest good representation of the source is a dipolar potential field bridging the neutral line between the H-alpha ribbons.

4. Pitch angle distributions for a trapped population (p>0) fit the ob-

served flux spectrum better than an isotropic distribution. The best fit appears to be with p=2, corresponding to a moderately anisotropic distribution with $N(\phi)=(\sin(\phi))^2$,

5. The flux spectrum can be fit reasonably well by the model, although the flat peak is not exactly reproduced. The model successfully predicts that at higher frequencies (f>5 GHz) the source appears double, and at lower frequencies (f<2 GHz) the source appears single.

Acknowledgements

Dr. M. Melozzi made the VLA maps of this flare and performed some of the early analysis of the data. We thank Dr. H. Zirin for providing us with Big Bear photographs. The VLA is operated by the National Radio Astronomy Observatory under contract with the National Science Foundation.

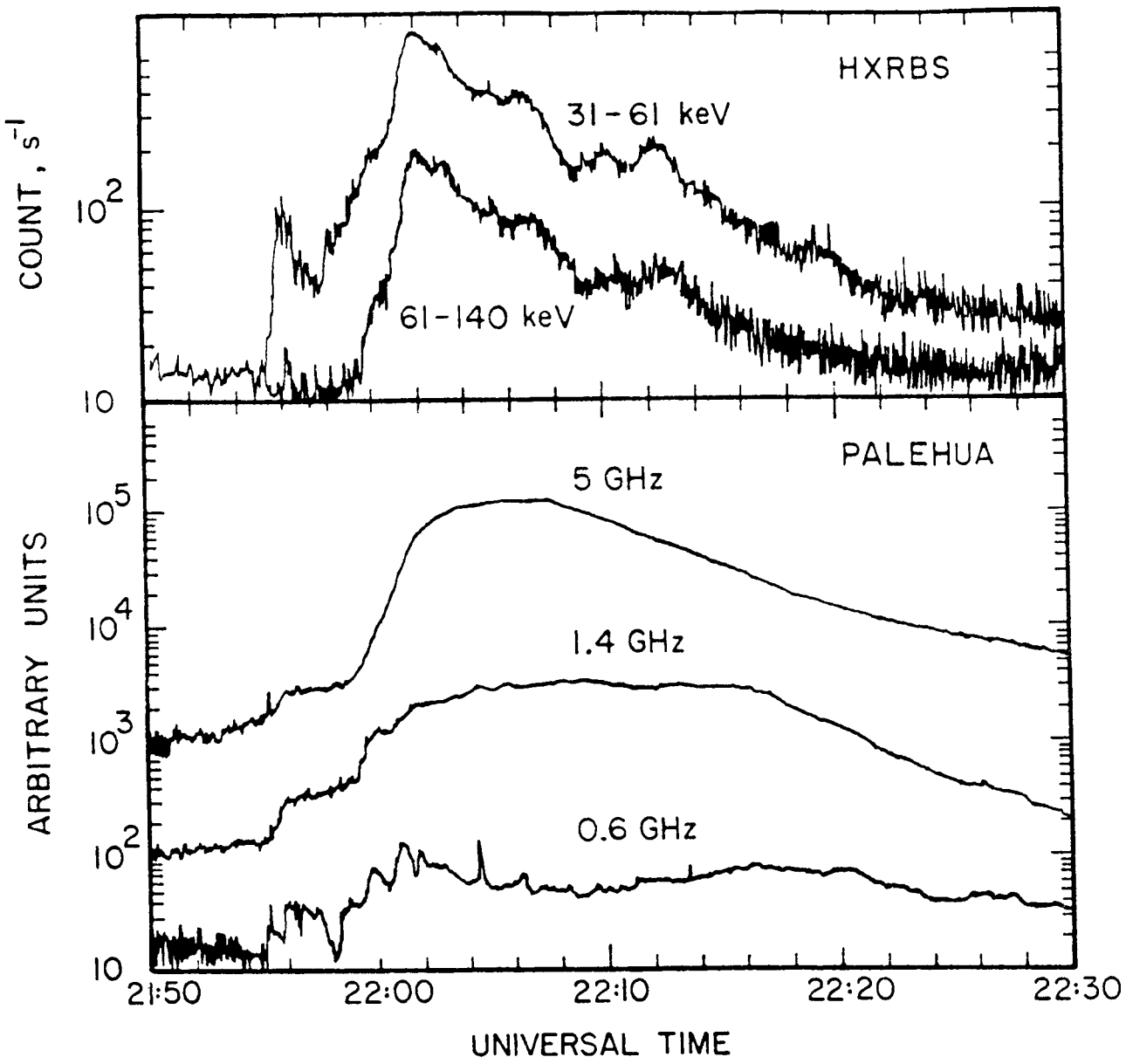

Fig. 1.

The two-ribbon, class 2B flare of 1981 November 14 was observed by HXRBS in x-rays with energies from 31 to 539 keV and in microwaves at the VLA and the patrol telescopes at Palehua.

a. HXRBS count-rate time profiles for the 31-61 keV and 61-140 keV channels and the corresponding spectral index.

b. Palehua single-dish observations at 4.995, 1.415 and 0.602 GHz. The first two frequencies (6 and 20 cm) are those used at the VLA for mapping this flare.

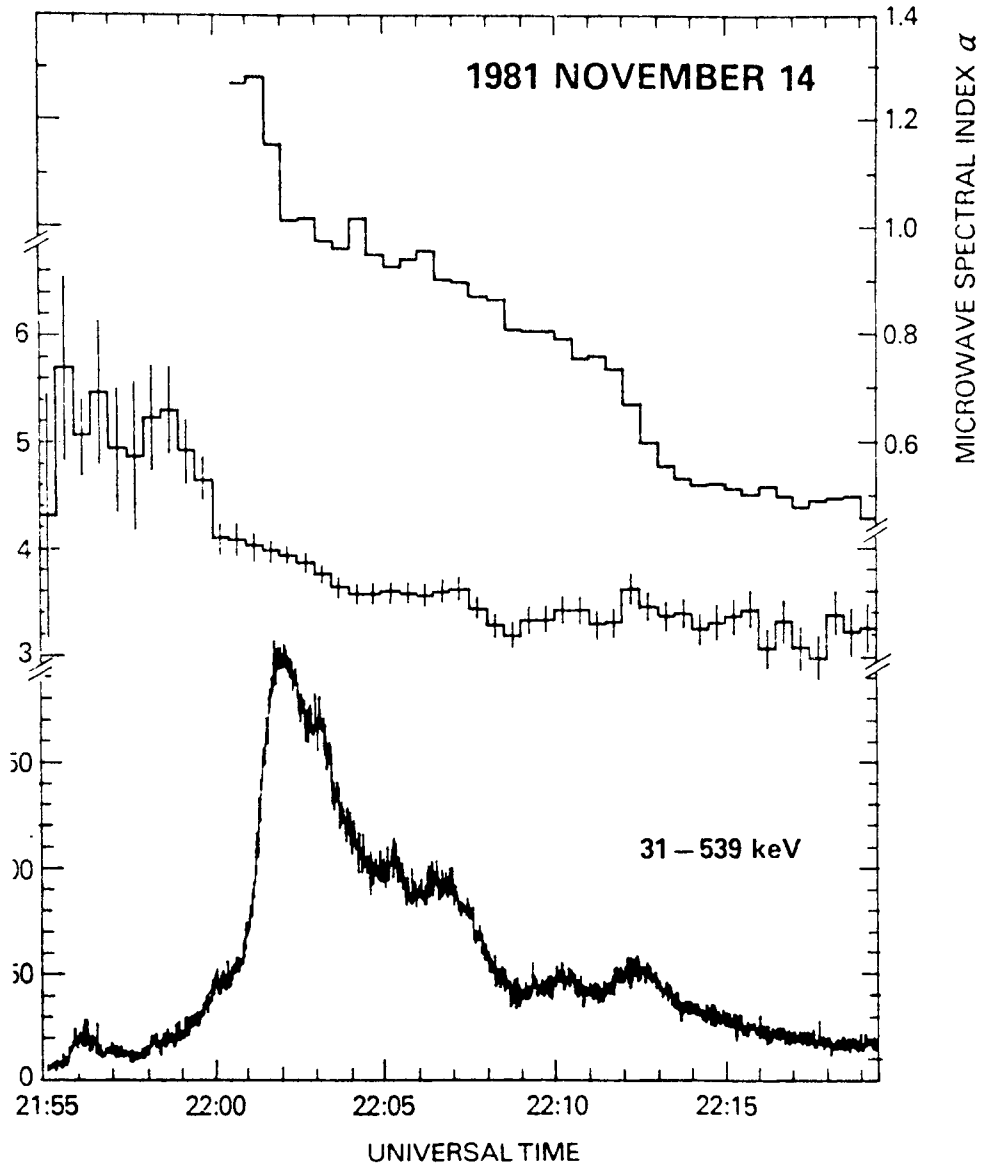

Fig. 2.

The HXRBS channels were fitted to a power law and the index γ plotted as a function of time. The time profile shows that the spectrum hardened from γ= 4.0 to about γ=3.3 starting from just before the x-ray maximum and continuing until at least 15 minutes afterwards.

The microwave patrol data were fitted to a double power law function, and the upper index α plotted as a function of time. Although this index is not strictly equal to the high frequency index of the microwaves, the profile shows that the spectrum hardened significantly and monotonically through the flare.

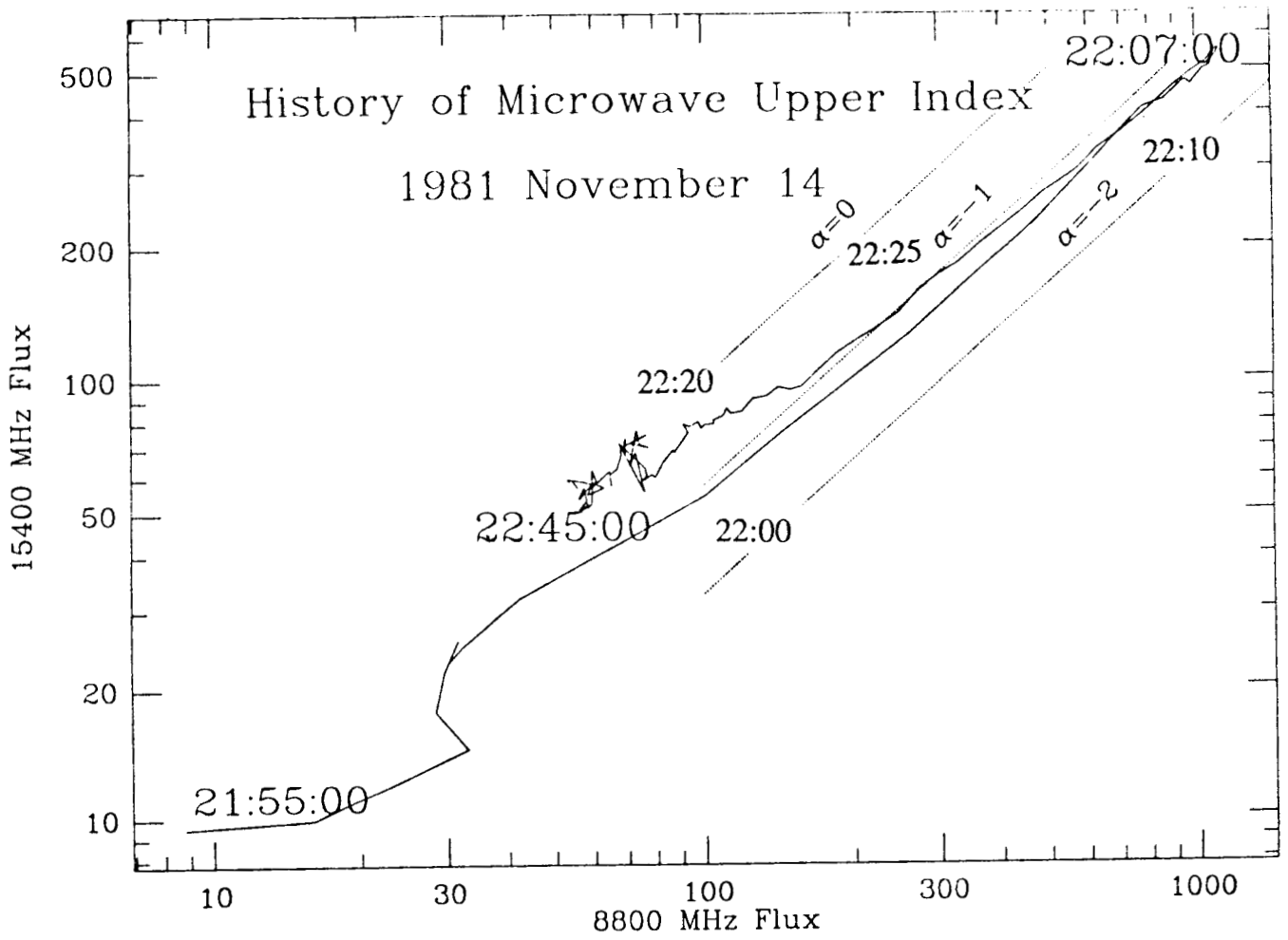

Fig. 3.

To show the evolution of the microwave spectral index, we have plotted the 8800 MHz flux against the 15400 MHz flux. This shows that, from shortly before the main hard x-ray peak to well after, the spectrum hardens steadily with the logarithmic slope α decreasing from -1.3 (at 22:02) to -0.5 (at 22:20). This index differs somewhat from that derived by the double power law fit (Fig. 2), but shows the same qualitative behavior.

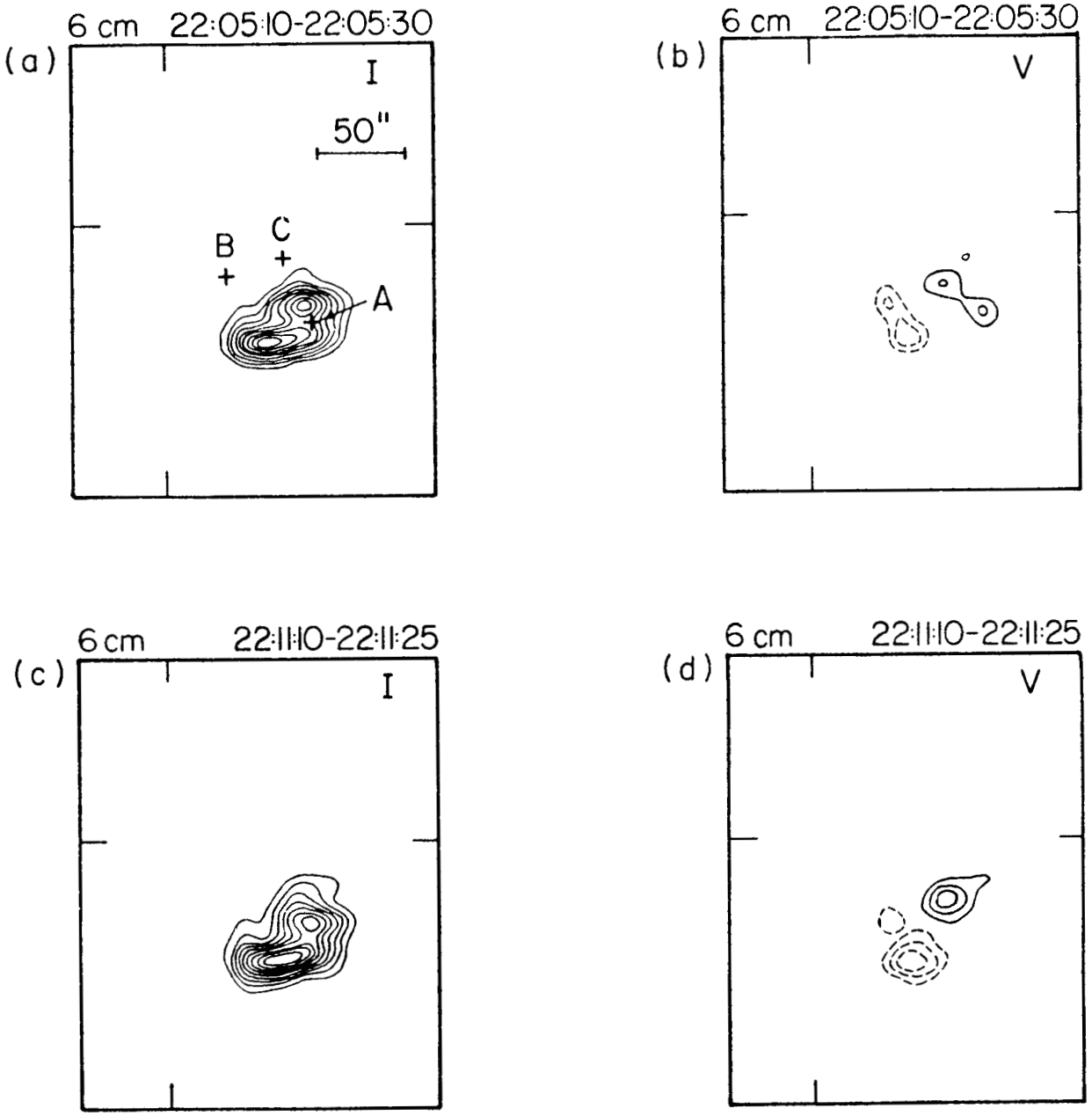

Fig. 4.

6 cm I and V VLA maps just after the main peak in hard x-rays. Note the two oppositely polarized peaks in the 6 cm map; these appear to straddle the Hα filament in the flaring region. The lowest contour in (a) and (c) is 8.1 x 10^6 K, and in (b) and (b) and (d) it is 4 x 10^6 and 6 x 10^6 K respectively. The contour intervals are the same as the base contour.

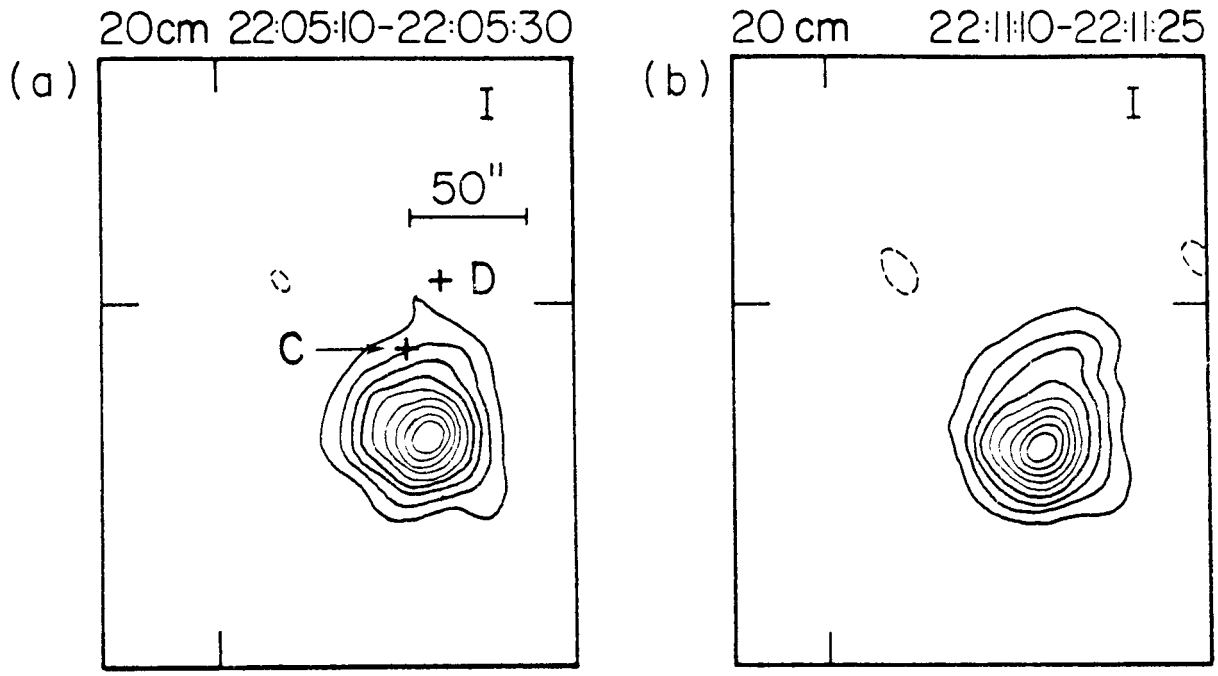

Fig. 5.

20 cm I and V VLA maps just after the main peak in hard x-rays. The 20 cm intensity source is single, with its location centered between the two 6 cm peaks (Fig. 4). The polarization map shows that the edges of the source are polarized in the same sense as the two 6 cm sources. The lowest contours are 1.7 x 10^7 K, 1.9 x 10^7 K, and 7.4 x 10^6 K in maps (a), (b) and (c), respectively. The contour intervals are the same as the base contour.

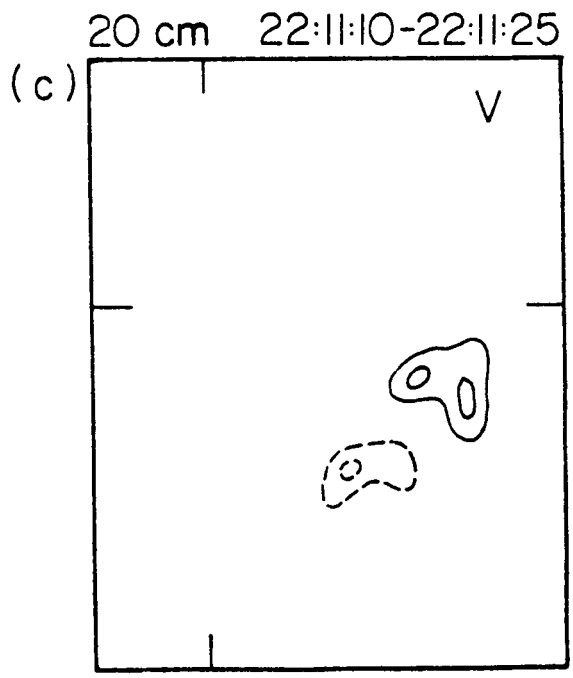

Fig. 6.

When the 20 cm map for 22:40 UT is overlain on the Hα photograph, the similarity is striking. We have made a 33" shift in position (away from the limb) of the 20 cm map (see dashed arrow) to align the Hα ribbons and the maxima of the microwave map. The shift corresponds to a projection effect with the height of the 20 cm sources 4-5 x 10^4 km above the Hα ribbons.

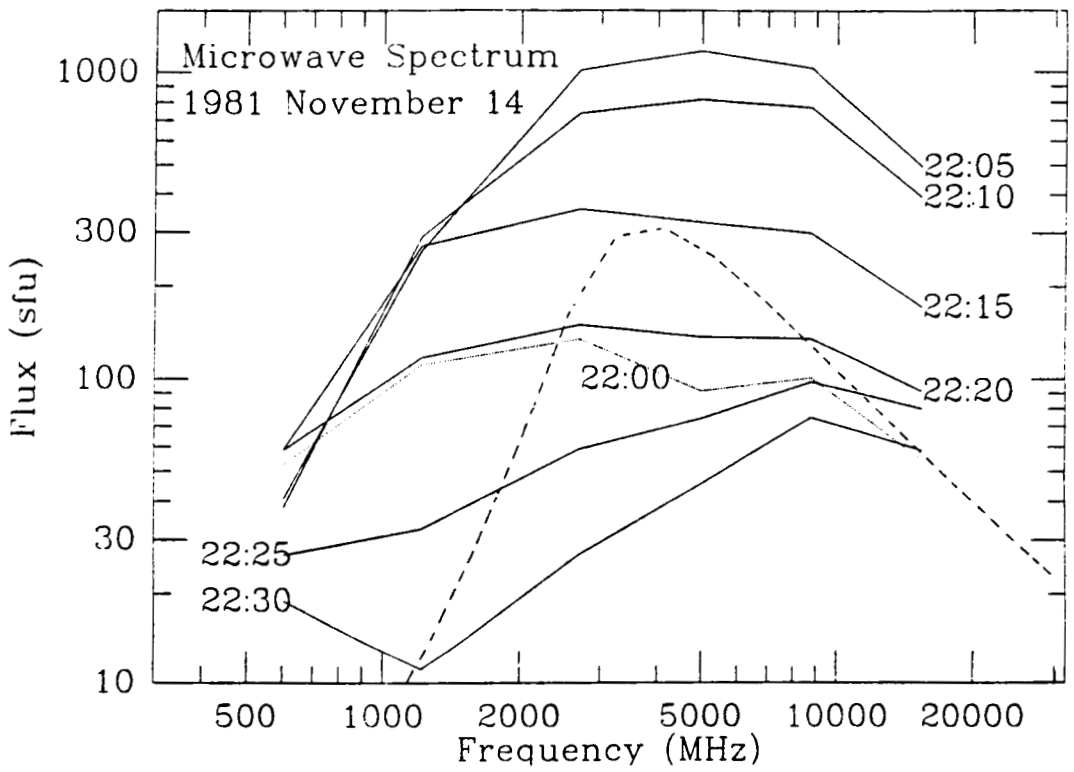

Fig. 7.

Microwave spectrum at selected times during the flare. Note the extreme breadth of the spectrum throughout the flare. For comparison, compare the overlay of a gyrosynchrotron spectrum of a homogeneous source. The breadth indicates that the source contains a wide range of magnetic field strengths, presumably in a system of loops trapping the electrons.

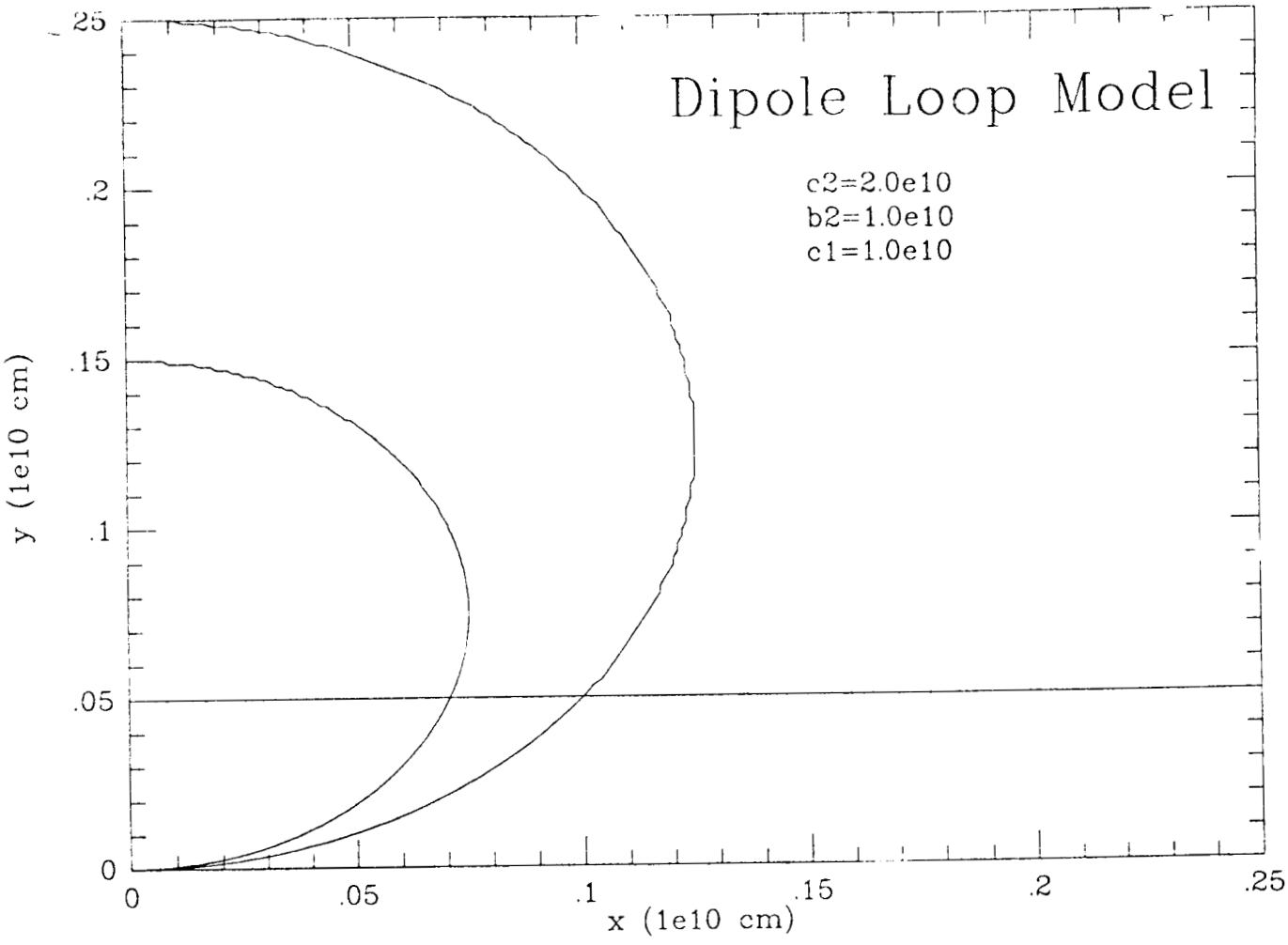

Fig. 8.

To account for the observed spectrum, we have computed gyrosynchrotron emission as a function of frequency from a model dipole loop with parameters esimated from the observations. The magnetic field is that due to a buried linear dipole. Typical values of the parameters are:

Apex height: $c2=2.0 \times 10^{10}$ cm

Inner height: $c1=1.0 \times 10^{10}$ cm

Footpoint separation: $b2=1.0 \times 10^{10}$ cm

Loop z-thickness: $a1=1.0 \times 10^{10}$ cm

The magnetic field strength at the footpoint is specified as a free parameter, but may be estimated from magnetograph observations.

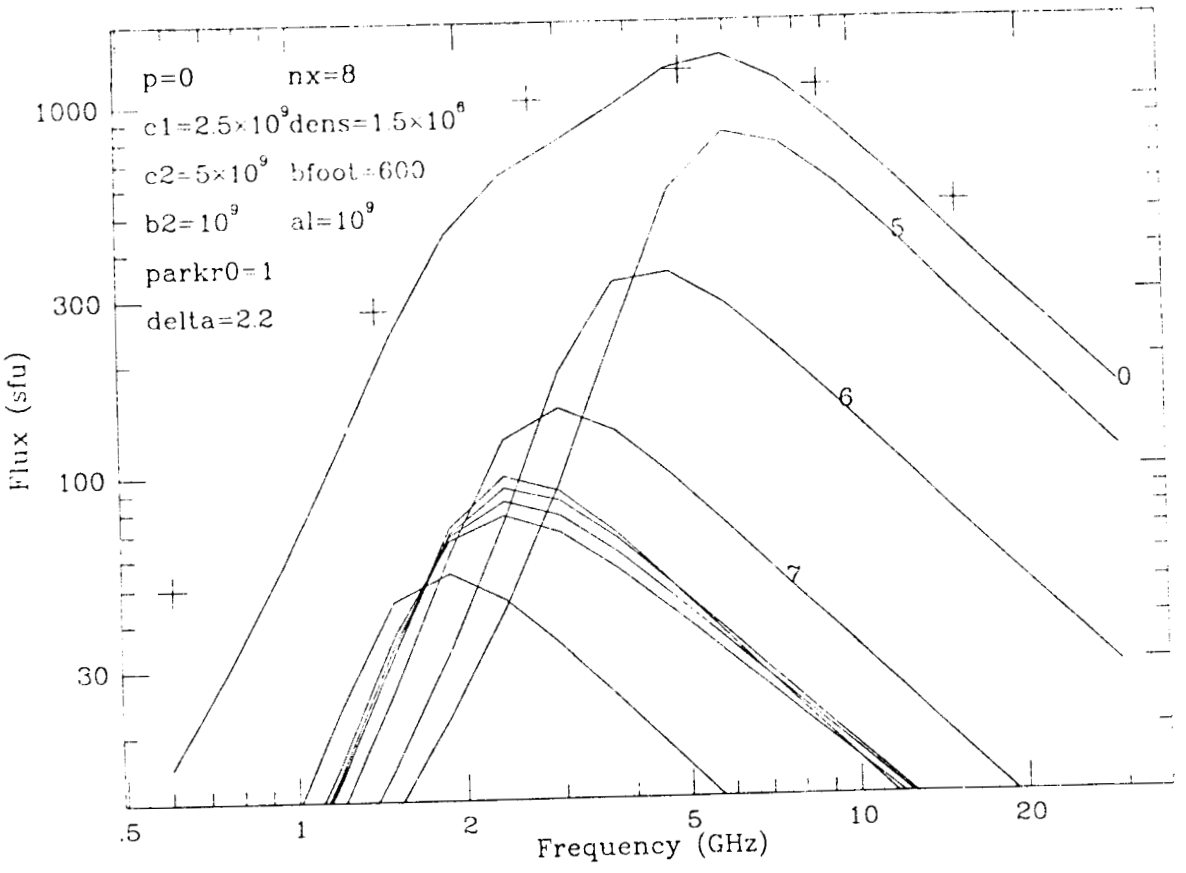

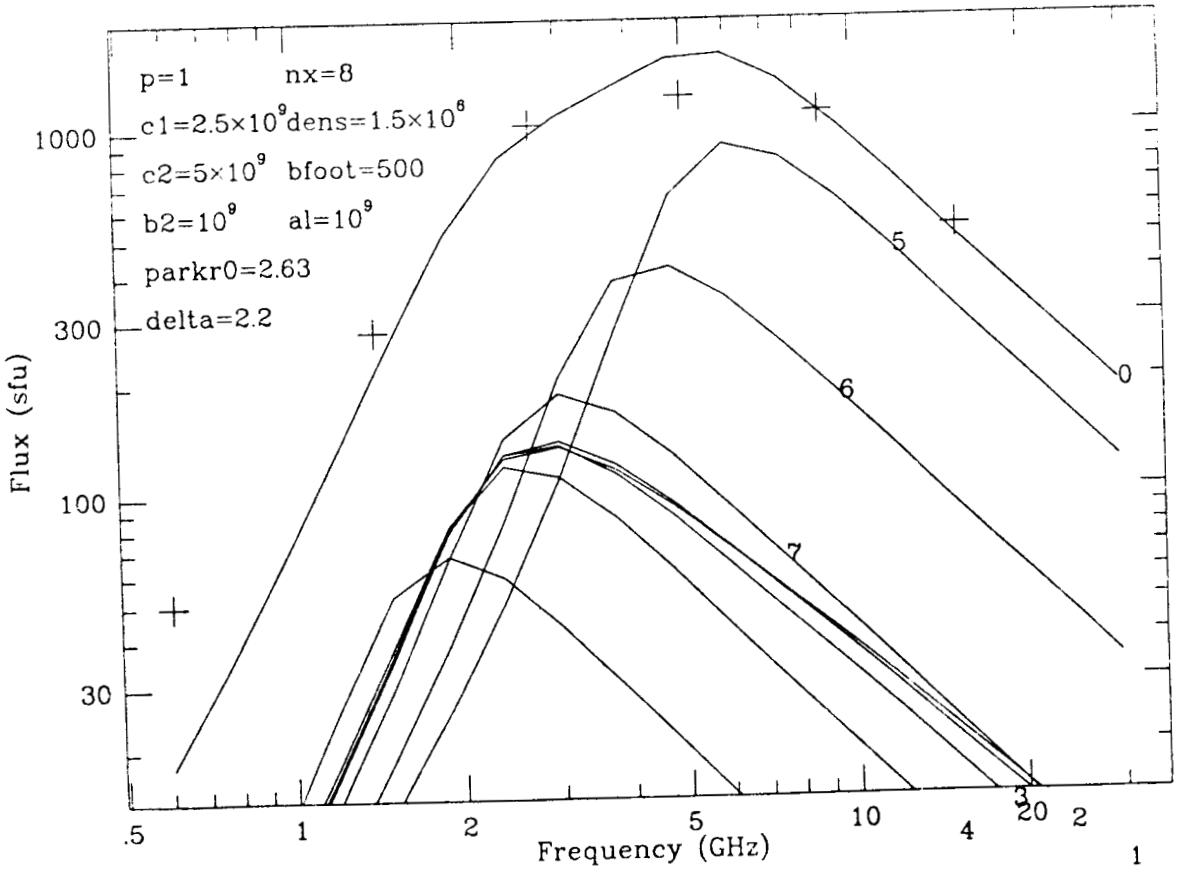

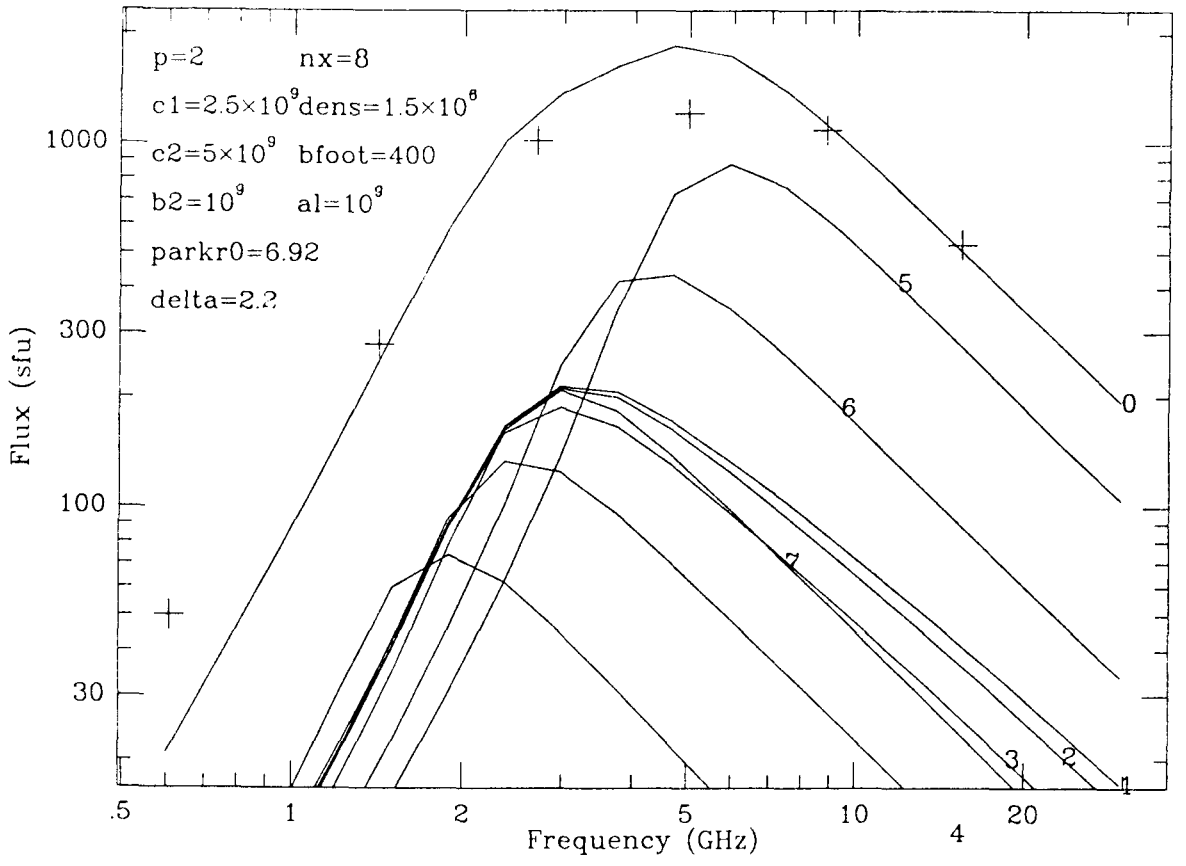

Fig. 9.

We have computed gyrosynchrotron spectra from the model loop system for a wide range of parameters, keeping the observable constraints in mind. The crosses show the Palehua flux at the flare maximum, 22:08:00 UT. The highest curve is the flux integrated over the entire loop, while the lower curves are the flux at selected points from the center outward toward the footpoints (1~center, 5~inner cusp of loop, 8~outer cusp of loop). In addition, we allowed the pitch angle distribution to depart from anisotropy, using the form:

$N(\phi)=(\sin(\phi))^p$, where p=0 corresponds to the isotropic case. For this kind of distribution, Parker (Phys. Rev. 107, 924, 1957) showed that the density of electrons in the loop is inversely proportional to the pth power of the magnetic field at that point.

a. p=0: Note how the top of the spectrum tilts to the left. This is due to the greater contribution from the inner cusp where B is large. In this case of isotropy, the electron density is constant along the lines of force.

b. p=1: In this case, as in c and d, the apex has a higher density than the legs of the loop. (parkr0=apex/foot density ratio.)

c. p=2: As p increases, the radiation becomes more highly beamed, and the contribution from the legs (curves 5,6) is relatively smaller.

C-4